On the giant sea-salt particles in the atmosphere

III. *An estimate of the production and distribution over the world ocean*[1]

By YOSHIAKI TOBA,[2] *The University of Chicago and Kyoto University*

(Manuscript received March 12, 1965)

ABSTRACT

Results of the preceding two parts of this series of articles, concerning the rate of production of giant particles at the sea surface and the manner in which they are distributed in the atmosphere, have been applied to marine climatic data to obtain estimated maps of the average distribution of giant sea-salt particles at the surface and at the 1-km level over the world ocean for the four seasons. The production rate and the number concentration, at the sea surface, of the particles of various class intervals of salt mass, and the number concentration at the 10-m and 2-km levels, are related to the above-mentioned maps.

1. Introduction

In part I[3] of this series, mechanisms that would govern the distribution of giant sea-salt particles in the atmosphere as a whole were studied by use of various observational data available from many references. In part II of this series, the vertical distribution of the particles in a boundary layer of 10-m thickness over the sea surface was analytically studied, and the effect of wind speed, humidity, etc., in the lowest atmosphere on the supply of particles to the overlying atmosphere was predicted. Since the most plausible rate of production of giant sea-salt particles at the sea surface was also determined in II as a function of wind speed at the 10-m level and the mass of salt in the particles, we may now combine all of these studies together with marine climatic data to estimate the average distribution of the particles at various levels over the world ocean.

The marine climatic data were obtained from wind force frequency distributions and mean humidities for various oceanic stations read or computed from charts of *U.S. Navy Marine Climatic Atlas of the World* (1955–1959). These are the principal independent variables based on the studies in II. The distribution of temperature and salinity of the sea water itself, which may have some effect on the production rate and size distribution of the particles, was not taken into account; in fact such effects cannot be considered because of insufficient study of them. The Arctic and the Antarctic Oceans were not included in this study, since conditions are more complicated there, and would require special study. This is the first edition of the estimated maps; as more advanced studies become available, it will be desirable to revise them.

2. Basic concepts in the calculation

The atmosphere may be divided into two parts: (1) the atmosphere as a whole, where it is assumed that the eddy diffusivity, etc., are vertically nearly constant, and convection, cloud formation, etc., occur; (2) a boundary layer of 10-m thickness over the sea surface, where there is no mean vertical motion of air, and the wind speed, the eddy diffusivity, the humidity, etc., sharply change with height. A discontinuity in the structure of the atmosphere at the 10-m level is a somewhat artificial concept, but is considered reasonable, in an approximate treatment.

[1] The research in this paper was sponsored by the Atmospheric Sciences Program, National Science Foundation, NSF grant G22292.

[2] Visiting Research Associate at the University of Chicago from Kyoto University for the period September 1963 to March 1965.

[3] For convenience the letters "I" and "II" are used in referring to the following two papers, respectively: Y. TOBA, On the giant sea-salt particles in the atmosphere. I. General features of the distribution, *Tellus*, **17**, No. 1 (1965); and II. Theory of the vertical distribution in the 10-m layer over the ocean, *Tellus*, **17**, No. 3 (1965).

TABLE 1. *Number concentration, $\theta_0(U_l,m)$, and production rate, $F_0(U_l,m)$, of giant sea-salt particles at the sea surface.*

Range of mass of salt (m : gm)	log m = 11.5–11	11–10.5	10.5–10	10–9.5	9.5–9	9–8.5	8.5–8	11.5–8	10–8
θ_0 (cm^{-3}) or F_0 (cm^{-2} sec^{-1}) for $U_l = 3$	θ_0 = .161	.0902	.0488	.0264	.0220	.0288	.0400	F_0 = .878	.800

Wind force at 10-m level	U_l = 0	1	2	3	4	5	6	7	8	9	10
Multiplication factor to be applied to above values of θ_0 or F_0	0	0	0	1	2.05	2.33	3.08	4.38	6.38	9.63	14.8

The average vertical distribution of the particles in the atmosphere as a whole over the sea was studied in I, and its characteristics were quantitatively explained by a combination of sedimentation, diffusion, convection processes, and coalescence in clouds. The average vertical distribution of number concentration of the particles, θ, was expressed by

$$\theta = \theta_l \exp(-\alpha z), \quad (1)$$

where θ_l is the value at the bottom of the atmosphere as a whole, i.e. the 10-m level, z is height above the 10-m level, and the value of α was determined as a function of the mass of salt, m, contained in a particle (Table 1 of I).

The equilibrium vertical distribution of the giant sea-salt particles in the 10-m layer was studied in II, and the vertical distribution of θ was expressed by

$$\log(\theta/\theta_0) = -m^{\frac{1}{3}} u_l^{-1} \chi(f_l, \gamma_l, z), \quad (2)$$

where θ_0 is the value at the sea surface, u_l the wind speed at the 10-m level, γ_l the friction factor, z height above the sea surface, and f_l a relative humidity difference defined by

$$f_l \equiv 98.23 - RH_l. \quad (3)$$

The figure 98.23 represents the equilibrium relative humidity for a solution of the salinity of sea water, and RH_l the relative humidity at the 10-m level. The value of χ was calculated in II as a function of f_l and z, for $\gamma_l^2 = 1.6 \times 10^{-3}$ which seems approximately valid for u_l from a few to 15 or 20 m sec^{-1} (Figs. 3 and 4 of II).

The most plausible values of $\theta_0(U_l,m)$, which were determined in II, are tabulated in Table 1 in the form used in the present calculation. The symbol U_l represents the wind force in the Beaufort scale. The production rate, $F_0(U_l,m)$, or upward flux of the particles per unit area at the sea surface is understood as

$$F_0 = \theta_0 / w_s, \quad (4)$$

where w_s represents the terminal velocity of sea-water droplets, i.e. droplets having a radius corresponding to a solution of the salinity of sea water, and the values are also entered in the last two columns of Table 1. Since for $U_l = 0$, 1, 2 the sea surface is smooth and no bubble entrainment or droplet production occurs, and since we are concerned with an equilibrium distribution, Table 1 indicates that the value of θ_0 is zero for these wind forces, although as a result of the past history of the air the actual value of θ_0 may not always be zero for these light winds.

The U.S. Navy Marine Climatic Atlas of the World (1955–1959) contains monthly charts of surface wind, surface air temperature, wet-bulb temperature and dew point. The data are entered for each of about 230 stations including ocean areas, ocean stations and coastal stations. From the surface wind charts, frequency distribution, $\phi(U_l)$, or percentage frequency of the occurrence for various wind forces, U_l, may be read. The average number concentration of the particles at the sea surface, $\bar{\theta}_0$, and the production rate, $\bar{F}_0$, may be calculated for each station by the equation:

$$\bar{\theta}_0(m) = \sum_{U_l} \theta_0(U_l, m)\, \phi(U_l)$$
$$\text{and} \quad \bar{F}_0(m) = \sum_{U_l} F_0(U_l, m)\, \phi(U_l). \quad (5)$$

The average number concentration of the particles at the 10-m level, $\bar{\theta}_l$, may be calculated for each station, by the use of equation (2), by

$$\bar{\theta}_l(m) = \sum_{U_l} \theta_0(U_l, m)\, \phi(U_l)\, 10^{-m^{\frac{2}{3}} u_l^{-1} \chi_l(f_l)}, \quad (6)$$

where the value of f_l may be obtained, for each station, from charts of air temperature and wet-bulb temperature or dew point. The average number concentration of the particles at various height levels, $\bar{\theta}_z$, may be calculated for each station by the use of equation (1), by

$$\bar{\theta}_z(m) = \bar{\theta}_l(m) \exp\{-\alpha(m) z\}. \quad (7)$$

In the following, the bars representing the average, will be omitted.

3. Calculation and maps of the estimated distribution

A three-month average of the frequency distribution of surface wind force, $\phi(U_l)$, was computed from data of the atlas for $U_l \leqslant 9$, for each station for each of the four seasons. Then the value of $\phi(10)$ was assigned by the equation:

$$\phi(10) = 100 - \sum_{U_l=0}^{9} \phi(U_l). \quad (8)$$

Although there is a possibility that wind forces greater than 10 have occurred, these were all included in $\phi(10)$, since we cannot know the values. There were some cases where the value of $\phi(10)$ in equation (8) had a small negative value because the value of $\phi(U_l)$ in the atlas for each month had no decimal. In this case the value of $\phi(10)$ was assigned zero.

A mean relative humidity was calculated from the median temperature and the median wet-bulb temperature for each station for each month. If there were no data of wet-bulb temperature, the median dew point was used. On rare occasions, the air temperature was below the freezing point; in these cases the relative humidity was determined from the saturation vapor pressure over supercooled water, not over ice, based on the study in II where equations (2) and (3) were introduced. From the average relative humidity for each month, a three-month average relative humidity for each of four seasons was computed for each station, whence the value of $\chi_l(f_l)$ was determined by equation (3), and Fig. 4 in II.

Computations of equations (5), (6) and (7), together with some of the above-mentioned derivations, were performed by the use of an electronic computer. In Figs. 1 through 8 are illustrated, as representative results, the computation of θ_0 for a class interval of mass of salt of $10^{-11.5}$–10^{-8} gm and $\theta_{1\,km}$ for that of 10^{-10}–10^{-8} gm for four seasons. Figures in the maps also represent the position of the stations. Figures showing values from coastal (island) stations are entered in parentheses. At some stations, especially those near the west coast of southern South America, some wind data are lacking in the atlas, and were supplemented by an interpolation between adjacent months, etc., and these results are also entered in parentheses.

Isolines were entered in Figs. 1 to 4 by placing the greatest weight on the figures without parentheses. The number of stations, however, was not sufficient to give detailed patterns of the isolines; so patterns of the isolines of percentage frequency of wind force 3 or less, which are the only isolines included in the surface wind chart of the atlas, were consulted to some extent, although the percentage frequency of wind force 3 or less cannot fully represent the wind data.

There are many stations which have no data of wet-bulb temperature or dew point. Values of $\theta_{1\,km}$ may not be obtained for these stations. In Fig. 9, are plotted the relation between $\theta_0(10^{-11.5}$–10^{-8} gm) and $\theta_{1\,km}(10^{-10}$–10^{-8} gm) for stations where both the wind and humidity data were available. Isolines in Figs. 5 to 8 were drawn by using the mean curve of Fig. 9 for stations of no humidity data.

In Fig. 10 are plotted relations among $\theta_0(10^{-11.5}$–10^{-8} gm), $\theta_{10\,m}(10^{-11.5}$–$10^{-8}$ gm), $\theta_{1\,km}(10^{-11.5}$–$10^{-8}$ gm) and $\theta_{2\,km}(10^{-11.5}$–$10^{-8}$ gm). In Fig. 11 are plotted relations among $\theta_{1\,km}(10^{-10}$–10^{-8} gm), $\theta_{10\,m}(10^{-10}$–10^{-8} gm) and $\theta_{2\,km}(10^{-10}$–10^{-8} gm). These relations may be used to obtain other values from the figures in Figs. 1 to 8.

The value of the production rate, F_0, of the particles at the sea surface may be obtained from Figs. 1 to 4 together with Table 1. For example, $F_0(10^{-11.5}$–10^{-8} gm) may be obtained by multiplying the figures in the maps by a factor $0.878/(0.161 + 0.0902 + \cdots + 0.0400) = 2.10$. The value of θ_0 for any class interval of salt mass

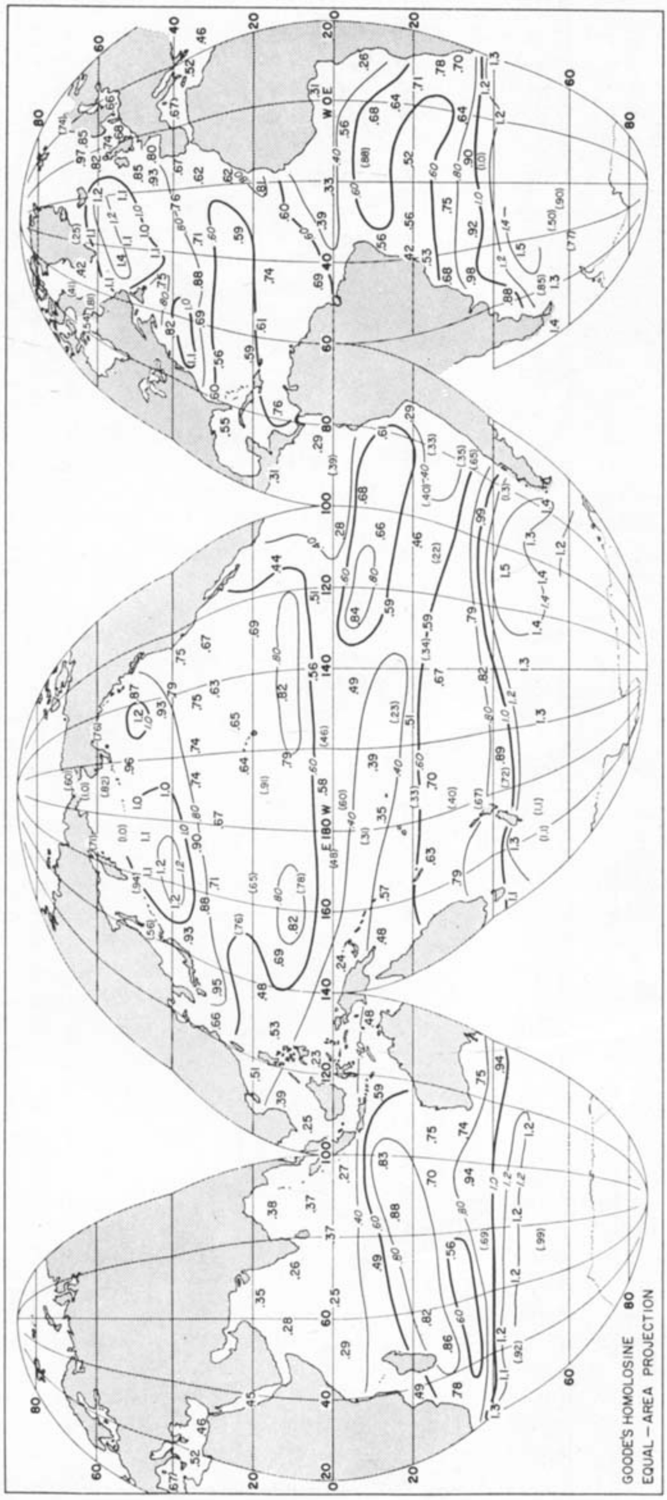

FIG. 1. Average number concentration of giant seasalt particles of the mass of salt ranging from $10^{-11.5}$ gm to 10^{-8} gm at the sea surface, $\theta_0(10^{-11.5}–10^{-8}$ gm) in cm^{-3}, March through May. Goode base map courtesy Department of Geography, the University of Chicago.

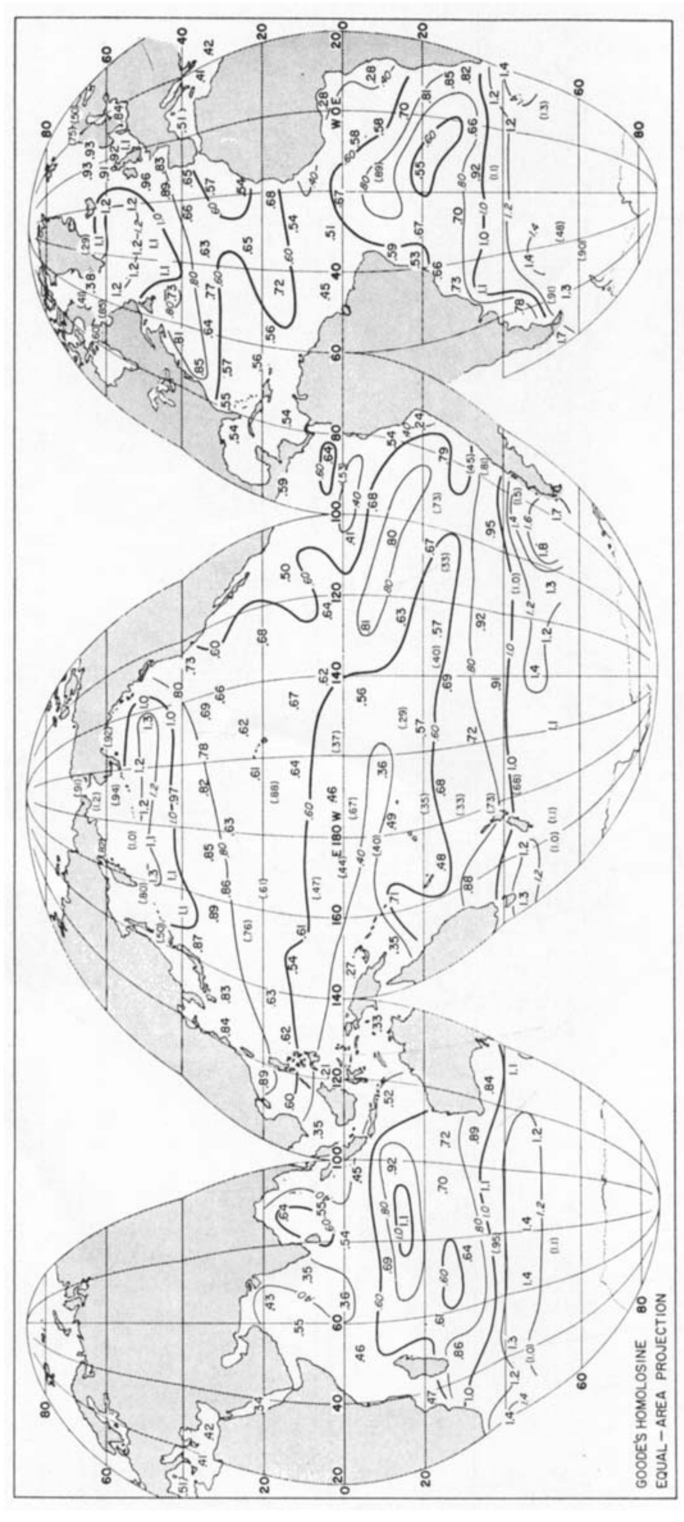

FIG. 2. Average number concentration of giant sea-salt particles in the mass of salt ranging from $10^{-11.5}$ gm to 10^{-8} gm at the sea surface, $\theta_0(10^{-11.5}$–10^{-8} gm) in cm^{-3}, June through August. Goode base map courtesy Department of Geography, the University of Chicago.

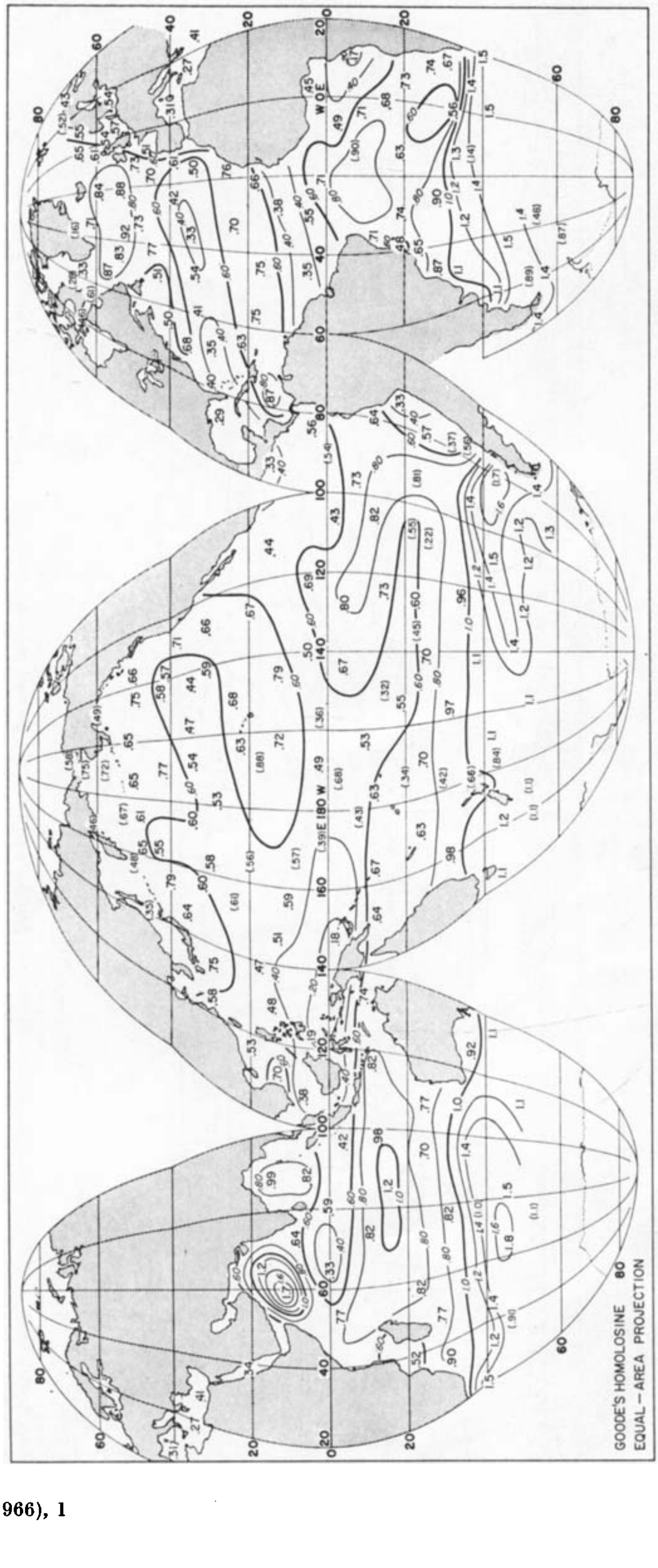

FIG. 3. Average number concentration of giant sea-salt particles of the mass of salt ranging from $10^{-11.5}$gm to 10^{-8} gm at the sea surface, $\theta_0(10^{-11.5}\text{–}10^{-8}$ gm) in cm^{-3}, September through November. Goode base map courtesy Department of Geography, the University of Chicago.

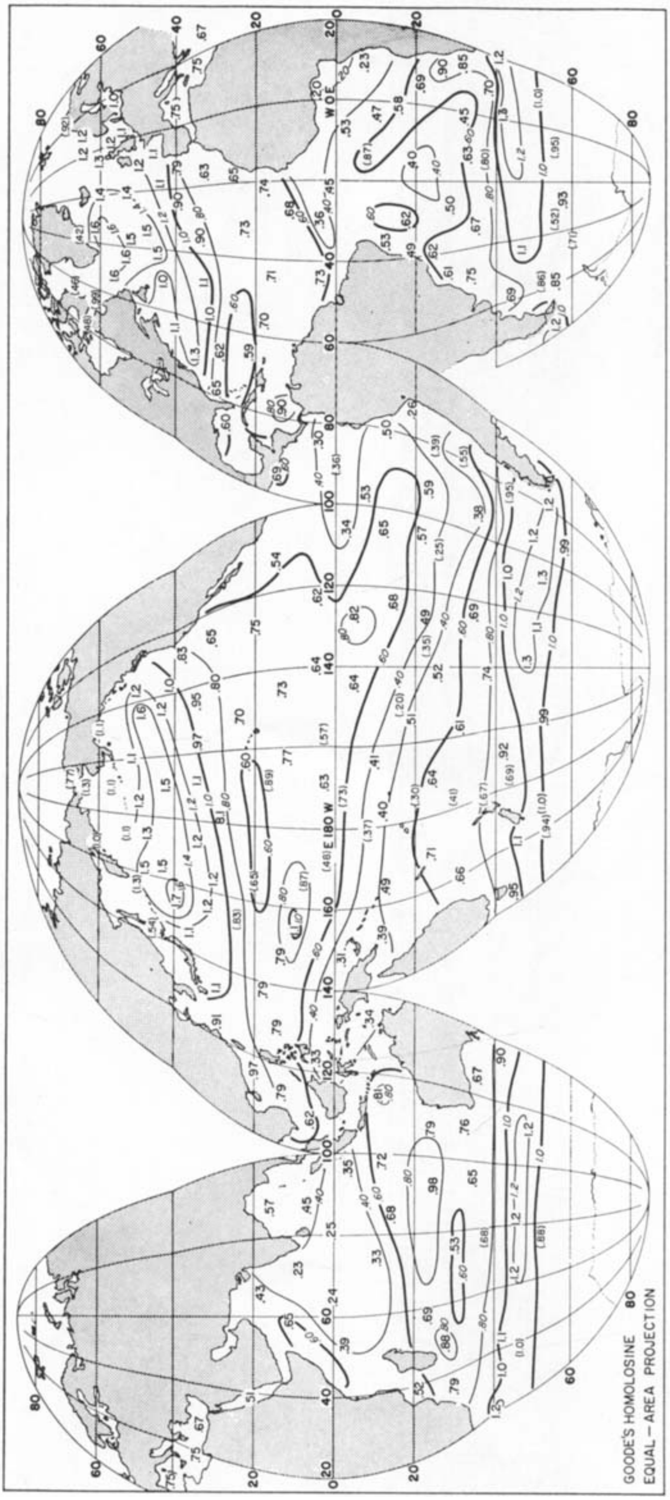

FIG. 4. Average number concentration of giant sea-salt particles of the mass of salt ranging from $10^{-11.5}$ gm to 10^{-8} gm at the sea surface, $\theta_0(10^{-11.5}$–10^{-8} gm) in cm^{-3}, December through February. Goode base map courtesy Department of Geography, the University of Chicago.

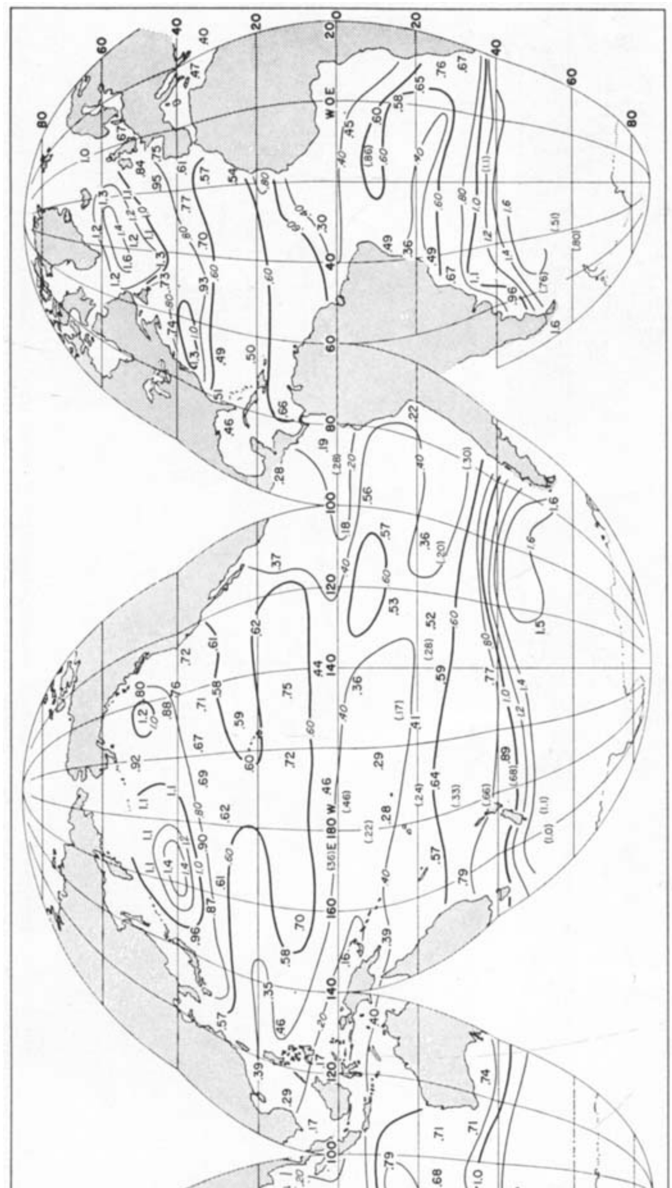

FIG. 5. Average number concentration of giant sea-salt particles of the mass of salt ranging from 10^{-10} gm to 10^{-8} gm at the 1-km level, $\theta_{1\,km}(10^{-10}-10^{-8}$ gm) in 10^{-2} cm^{-3}, March through May. Goode base map courtesy Department of Geography, the University of Chicago.

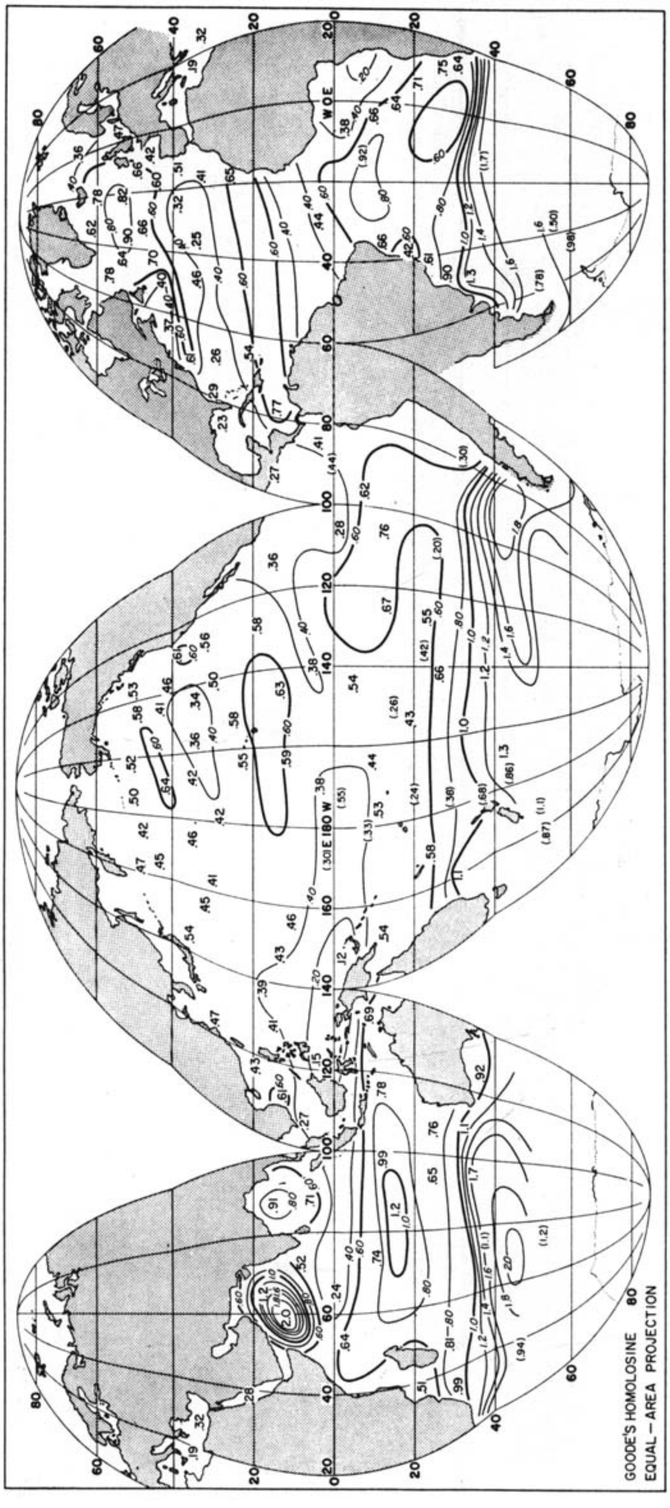

FIG. 6. Average number concentration of giant sea-salt particles of the mass of salt ranging from 10^{-10} gm to 10^{-8} gm at the 1-km level, $\theta_{1\,km}$ (10^{-10}–10^{-8} gm) in 10^{-2} cm^{-3}, June through August. Goode base map courtesy Department of Geography, the University of Chicago.

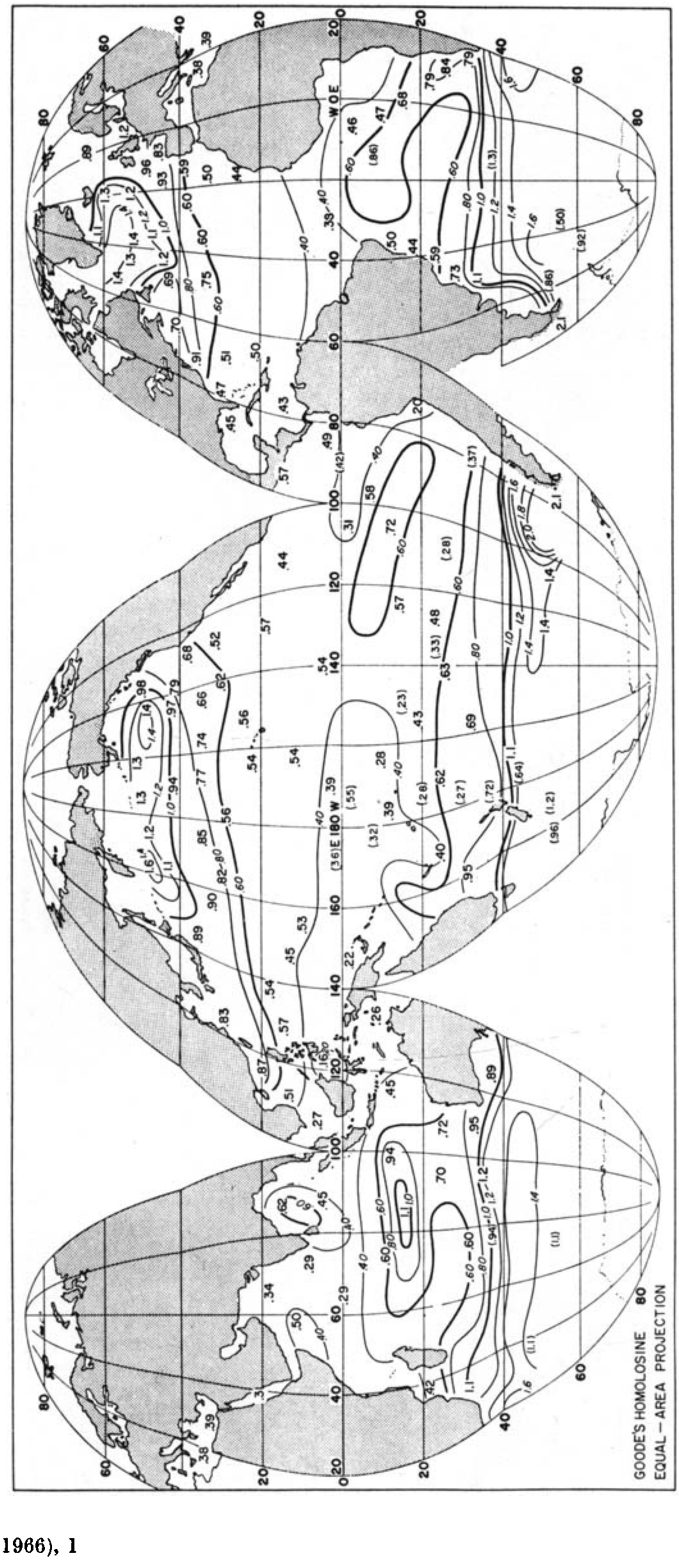

FIG. 7. Average number concentration of giant sea-salt particles of the mass of salt ranging from 10^{-10} gm to 10^{-8} gm at the 1-km level, $\theta_{1\,km}(10^{-10}$–10^{-8} gm) in 10^{-2} cm^{-3}, September through November. Goode base map courtesy Department of Geography, the University of Chicago.

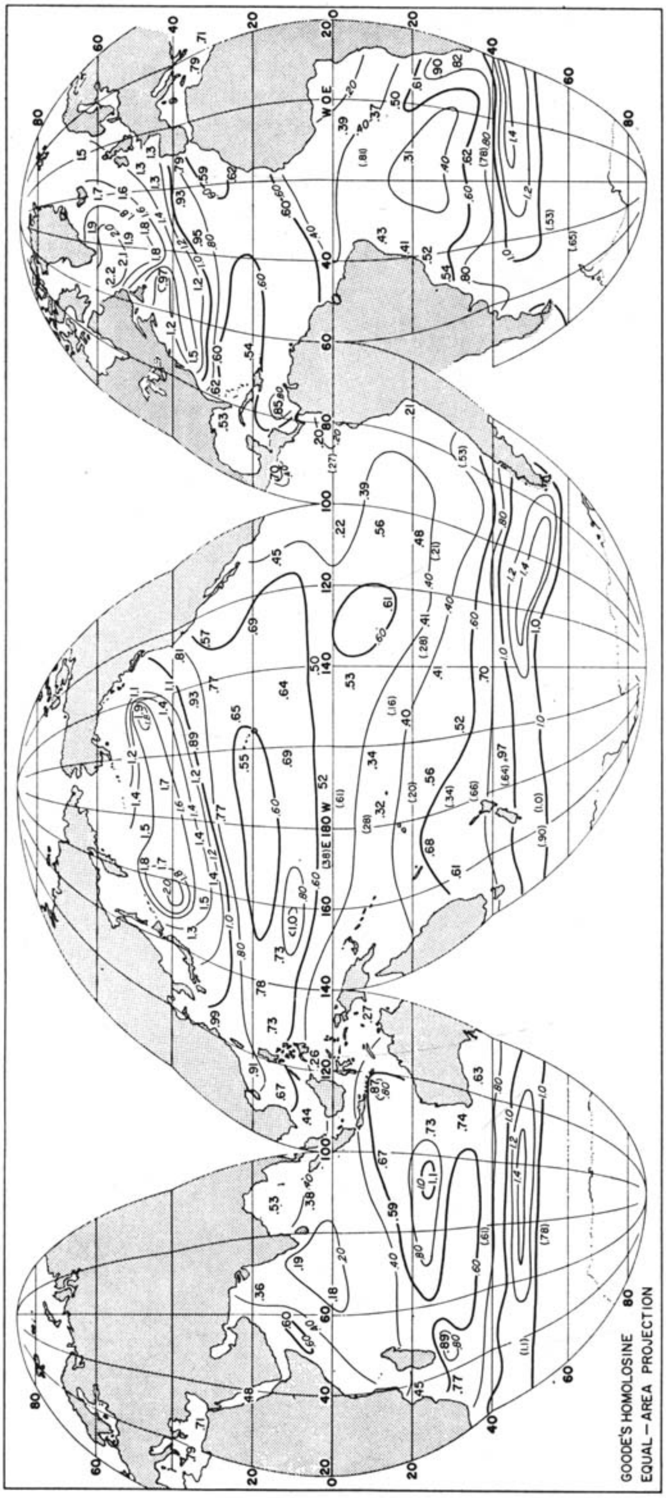

Fig. 8. Average number concentration of giant sea-salt particles of the mass of salt ranging from 10^{-10} gm to 10^{-8} gm at the 1-km level, $\theta_{1\,km}$ (10^{-10}–10^{-8} gm) in 10^{-2} cm^{-3}, December through February. Goode base map courtesy Department of Geography, the University of Chicago.

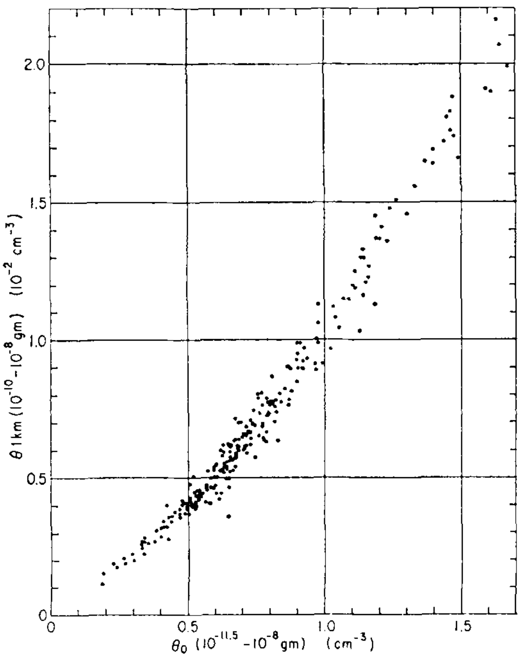

FIG. 9. Relation between $\theta_0(10^{-11.5}$–10^{-8} gm) and $\theta_{1\,km}(10^{-10}$–10^{-8} gm).

may be obtained in the same way, and the value of F_0 for any class interval of mass may be obtained from these θ_0 values and equation (4). The value of $\theta_{10\,m}$, $\theta_{1\,km}$, $\theta_{2\,km}$ and $\theta_{3\,km}$ for various class intervals were computed in the course of the present calculation, but they are not included in this paper.

The three-month average relative humidity for each station was 93% in maximum and 63% in minimum, and almost all values fell between 90% and 70%; consequently the range of the value of χ_l was from 4.0 to 7.2 (10^8 gm$^{-\frac{1}{3}}$ cm sec^{-1}). This means that the average number concentration of the particles of smaller mass of salt (down to $m = 10^{-11.5}$ gm) is almost entirely determined by wind. Thus the points in Fig. 10 fall in a very narrow range. The average number concentration of the particles of about 10^{-10} gm is influenced to some extent by the humidity distribution, so the points in Fig. 9 are more scattered than in Fig. 10. Average number concentrations of the particles of 10^{-9} gm or larger are very much influenced by the humidity distribution. These relations may also be understood from Figs. 5, 6, 7 and Table 6 of II.

An error which entered in determining $\phi(10)$ by equation (8) seemed usually less than 0.1 cm^{-3} in values of $\theta_0(10^{-11.5}$–10^{-8} gm), but errors entered in the values of $\theta_0(U_l,m)$ and $\chi_l(f_l)$ for stronger wind forces, such as 9 and 10, might be larger than this. Since the distribution of the particles near the coast of a continent may not always be assumed as an equilibrium distribution, isolines were not continued up to the very coast. It is also interesting to see that figures at island or coastal stations generally deviate from the main trend in oceanic stations.

From Figs. 1 to 8, the following features of the global distribution are recognizable. In winter there are maxima of 1.6 cm^{-3} in $\theta_0(10^{-11.5}$–10^{-8} gm) and 2.0×10^{-2} cm^{-3} in $\theta_{1\,km}(10^{-10}$–10^{-8} gm) to the east of Japan and to the west of Canada in the Pacific Ocean, and to the east of Canada (40°–60° N) in the Atlantic Ocean. In summer these maxima almost disappear and the concentration falls off to about 0.8–0.9 cm^{-3}

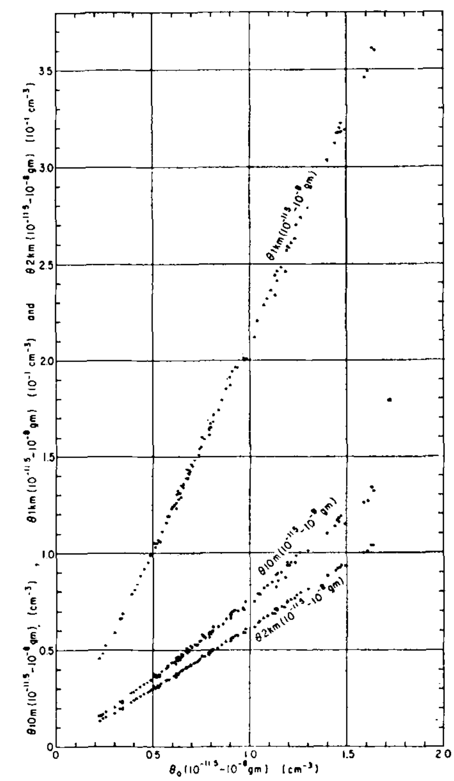

FIG. 10. Relations among $\theta_0(10^{-11.5}$–10^{-8} gm), $\theta_{10\,m}(10^{-11.5}$–$10^{-8}$ gm), $\theta_{1\,km}(10^{-11.5}$–$10^{-8}$ gm) and $\theta_{2\,km}(10^{-11.5}$–$10^{-8}$ gm).

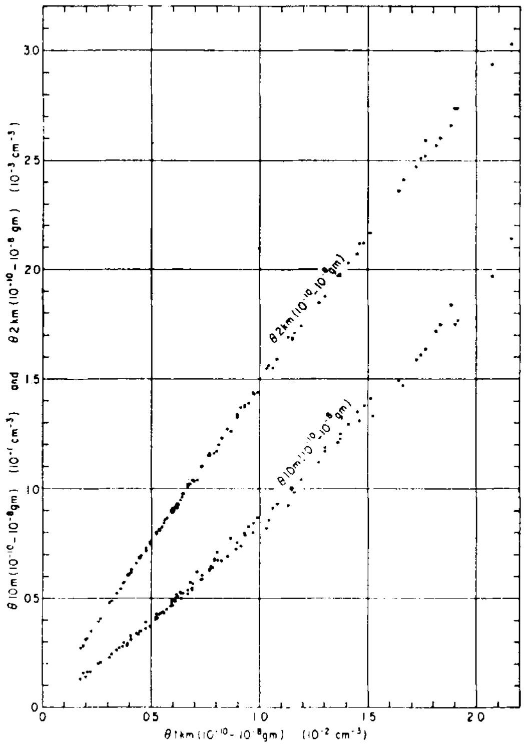

FIG. 11. Relations among $\theta_{1\,km}(10^{-10}\text{–}10^{-8}$ gm), $\theta_{10\,m}(10^{-10}\text{–}10^{-8}$ gm), and $\theta_{2\,km}(10^{-10}\text{–}10^{-8}$ gm).

in $\theta_0(10^{-11.5}\text{–}10^{-8}$ gm) and about 0.6×10^{-2} to 0.9×10^{-2} cm^{-3} in $\theta_{1\,km}(10^{-10}\text{–}10^{-8}$ gm). In spring and autumn, small maxima of about 1.2 to 1.4 cm^{-3} in $\theta_0(10^{-11.5}\text{–}10^{-8}$ gm) and about 1.4×10^{-2} to 1.6×10^{-2} cm^{-3} in $\theta_{1\,km}(10^{-10}\text{–}10^{-8}$ gm) appear in these areas. In the southern oceans between 40° S and 60° S, there are always maxima and the values are 1.2 to 1.3 cm^{-3} and 1.4×10^{-2} cm^{-3} in summer, and 1.6 to 1.8 cm^{-3} and perhaps 1.8×10^{-2} to 2.0×10^{-2} cm^{-3} in winter for $\theta_0(10^{-11.5}\text{–}10^{-8}$ gm) and $\theta_{1\,km}(10^{-10}\text{–}10^{-8}$ gm), respectively; the annual variation in the southern hemisphere is generally small. There is an area of minimum concentration of 0.20 to 0.30 cm^{-3} in $\theta_0(10^{-11.5}\text{–}10^{-8}$ gm) and 1.2×10^{-3} to 2.7×10^{-3} cm^{-3} in $\theta_{1\,km}(10^{-10}\text{–}10^{-8}$ gm) in the area of Indonesia to New Guinea the year round. Another conspicuous feature is that a maximum of 1.7 cm^{-3} in $\theta_0(10^{-11.5}\text{–}10^{-8}$ gm) and 2.0×10^{-2} cm^{-3} in $\theta_{1\,km}(10^{-10}\text{–}10^{-8}$ gm) appears in the western part of the Arabian Sea in summer.

4. Concluding remarks

It has been deduced that the average geographical distribution of the giant sea-salt particles, in the atmosphere as a whole over the oceans is primarily determined by the distribution of surface wind, if we take a range of the mass of salt contained in the particles down to $10^{-11.5}$ gm. If we take the range of the mass of salt larger than 10^{-10} gm, the distribution is also influenced by humidity distribution near the sea surface.

If the frequency of stronger winds increases, the average distribution will be much influenced. The present estimate is restricted to a calculation of an average condition based on the assumption of equilibrium distribution. Consequently, it has a significance only in a climatological sense. Problems left for future consideration are those of the variation about the average, and of the adjustment of the distribution to a change in wind, and thereby to a change in the flux of the particles at the sea surface. Especially in some extreme cases, such as in a typhoon or hurricane, the production rate of particles at the sea surface and the vertical distribution in the lowest atmospheric layer will need a completely different treatment. The production and distribution of the particles in the Arctic and the Antarctic Oceans will also need a special study because of the low temperature and the presence of ice.

The distribution of giant sea-salt particles over the continents may be estimated, to some extent, by use of the present estimate over the oceans and by means of the study in I, together with some wind-distribution data over the continents. Further studies, however, on the ground sink, rainout, etc., would seem to be necessary.

The circulation of particles, i.e., their actual net flux from the sea surface to the cloud, and back again to the earth's surface, will need additional study, since the present study concerns only the equilibrium distribution. The most interesting and important problem, however, which might be now undertaken from the present survey, would be to elucidate the role this system of distribution of giant sea-salt particles plays in meteorological phenomena over the earth.

Acknowledgments

The present study was performed at the Cloud Physics Laboratory of the University of Chicago under the supervision of Professor Horace R. Byers. He arranged the author's visit to the United States, gave constant advice, suggestions, discussed problems with the author, and kindly corrected the author's sentences. The author wishes to express his profound thanks to Professor Byers. He also thanks Dr. Takashi Murayama of the Enrico Fermi Institute for Nuclear Studies, the University of Chicago, who very much helped him on the use of an electronic computer, and other members of the author's laboratory who helped in and discussed various parts of his work. Special thanks are due to Professor Shōitirō Hayami of the Geophysical Institute, Kyoto University, Japan, who permitted the author to visit the United States on leave of absence, and who, with other members of his laboratory, gave continuous encouragement.

REFERENCES

TOBA, Y., 1965, On the giant sea-salt particles in the atmosphere. I. General features of the distribution. *Tellus*, **17**, pp. 131–145.

TOBA, Y., 1965, On the giant sea-salt particles in the atmoshpere. II. Theory of the vertical distribution in the 10-m layer over the ocean. *Tellus*, **17**, pp. 365–382.

U.S. NAVY, 1955–1959, *Marine Climatic Atlas of the World*, Vols. I–V, Washington, D.C., Government Printing Office.

WOODCOCK, A. H., 1953, Salt nuclei in marine air as a function of altitude and wind force. *J. Met.*, **10**, pp. 362–371.